ARTICLES SCIENCE CHINA Materials

mater.scichina.com link.springer.com

Published online 8 June 2018 | https://doi.org/10.1007/s40843-018-9293-8
*Sci China Mater* 2019, 62(2): 256–272

# *In vitro* and *in vivo* investigation on biodegradable Mg-Li-Ca alloys for bone implant application

Dandan Xia[1], Yang Liu[2], Siyi Wang[1], Rong-Chang Zeng[3], Yunsong Liu[1,4*], Yufeng Zheng[2*] and Yongsheng Zhou[1,4]

**ABSTRACT** **Magnesium alloys show promise for application in orthopedic implants, owing to their biodegradability and biocompatibility. In the present study, ternary Mg-(3.5, 6.5 wt%) Li-(0.2, 0.5, 1.0 wt%) Ca alloys were developed. Their mechanical strength, corrosion behavior and cytocompatibility were studied. These alloys showed improved mechanical strength than pure Mg and exhibited suitable corrosion resistance. Furthermore, Mg-3.5Li-0.5Ca alloys with the best *in vitro* performance were implanted intramedullary into the femurs of mice for 2 and 8 weeks. *In vivo* results revealed a significant increase in cortical bone thickness around the Mg-3.5Li-0.5Ca alloy rods, without causing any adverse effects. Western blotting and immunofluorescence staining of β-catenin illustrated that Mg-3.5Li-0.5Ca alloy extracts induced osteogenic differentiation of human bone marrow-derived mesenchymal stem cells (hBMMSCs) through the canonical Wnt/β-catenin pathway. Our studies demonstrate that Mg-3.5Li-0.5Ca alloys hold much promise as candidates for the facilitation of bone implant application.**

**Keywords:** Mg-Li-Ca alloy, cytocompatibility, biocompatibility, human bone marrow-derived mesenchymal stem cells, osteogenic differentiation

## INTRODUCTION

Magnesium (Mg) alloys show promise for application in orthopedic implants, owing to their biodegradability in human physiological conditions. Unlike permanent metals and absorbable polymers, magnesium alloys exhibit a favorable balance between degradation and strength. Moreover, Mg is a natural ion with multiple functions in biological systems. Indeed, several *in vivo* studies have shown that magnesium alloys could be used as potential degradable implant biomaterials [1–4].

However, there are problems associated with the application of pure Mg as load-bearing orthopedic implant materials. For example, pure Mg has low mechanical strength, which limits its application after implantation in the human body [1,5]. The second concern is that pure Mg is easily biodegradable and degrades rapidly in the human body; during this process mechanical integrity is lost before new bone is fully regenerated [6]. For these reasons, the development of new magnesium alloys with improved mechanical strength and enhanced corrosion resistance is highly desirable.

Alloying is one of the most effective ways to improve the corrosion properties and mechanical strength of pure Mg. Magnesium alloys have been widely applied, such as LAE442 (Mg-4Li-4Al-2RE) and AZ91D (Mg-9Al-1Zn) [1,2,7]. However, these alloys contain high quantities of aluminium (Al) and rare earth elements, which are associated with potential toxic effects on the human body [8]. Therefore, it is highly desirable to develop magnesium alloys with more biocompatible alloying elements, such as zinc (Zn), calcium (Ca), manganese (Mn), lithium (Li), and strontium (Sr).

Among these alloying elements, Li can change the hexagonal close packed (hcp) structure of Mg into body centered cubic (bcc). Mg-Li alloys can be classified into three types, depending on the lithium content: α-phase (0 to 5 wt% Li), dual phase (α+β; 5 to 10.3 wt% Li), and β-phase (>10.3 wt% Li) [9]. Previous studies have reported that Mg-Li-based alloys are more corrosion resistant than Mg-based alloys [9]. Moreover, incorporation of Li in

[1] Department of Prosthodontics, Peking University School and Hospital of Stomatology, Beijing 100081, China
[2] Department of Materials Science and Engineering, College of Engineering, Peking University, Beijing 100871, China
[3] College of Materials Science and Engineering, Shandong University of Science and Technology, Qingdao 266590, China
[4] National Engineering Laboratory for Digital and Material Technology of Stomatology, National Clinical Research Center for Oral Diseases, Beijing Key Laboratory of Digital Stomatology, Beijing 100081, China
* Corresponding authors (emails: kqliuyunsong@163.com (Liu Y); yfzheng@pku.edu.cn (Zheng Y))

  

**Table 1** Analyzed compositions of the Mg-Li-Ca alloys

| Nominal composition (wt%) | Analyzed composition (wt%) | | |
|---|---|---|---|
| | Li | Ca | Mg |
| Mg-3.5Li-0.2Ca | 4.2 ± 0.1 | 0.31 ± 0.03 | Balance |
| Mg-3.5Li-0.5Ca | 3.8 ± 0.1 | 0.53 ± 0.04 | Balance |
| Mg-3.5Li-1.0Ca | 3.7 ± 0.1 | 1.03 ± 0.03 | Balance |
| Mg-6.5Li-0.2Ca | 7.0 ± 0.2 | 0.28 ± 0.02 | Balance |
| Mg-6.5Li-0.5Ca | 6.5 ± 0.1 | 0.39 ± 0.03 | Balance |
| Mg-6.5Li-1.0Ca | 6.7 ± 0.1 | 0.79 ± 0.06 | Balance |

Mg-Li alloy can reduce the density of magnesium alloys. From a biomedical perspective, Li was approved by the US Food and Drug Administration (FDA) to treat bipolar and depressive disorders for up to 50 years [10,11]. Indeed, reports indicate that $Li^+$ ions can promote bone formation and enhance bone density *in vivo* [12–14].

Incorporation of Ca into Mg-Li-based alloys results in more refined microstructures, thus improving mechanical strength [15,16], and Ca can improve the corrosion properties of Mg-Li alloys [17,18]. Furthermore, Ca is considered as one of the most important factors in normal bone development and is one of the major elements in bone [19,20].

Preliminary studies have been conducted on the corrosion behavior of Mg-Li-Ca alloys [21,22]. However, there are no reports related to their biocompatibility *in vitro* or *in vivo*. Therefore, in the present study, the influence of Mg-Li-Ca alloys on the differentiation of hBMMSCs was explored. Meanwhile, the *in vivo* performance of Mg-Li-Ca alloy when implanted into an animal model was assessed. Furthermore, the potential mechanism of osteogenic differentiation around the Mg-Li-Ca alloys was investigated.

## EXPERIMENTAL SECTION

### Materials preparation and microstructural characterization

Mg-(3.5, 6.5 wt%)Li-(0.2, 0.5, 1.0 wt%)Ca alloys were melted and cast by using commercial magnesium, pure Li, and pure Ca. The analyzed compositions are shown in Table 1. High purity Mg (99.95%) was used in a control group. Ingots of the alloys and pure Mg were extruded at 280°C with a reduction ratio of 16 into bars. The samples were cut to a dish-shaped size ($\Phi$10 × 2 mm) for microstructural characterization, corrosion measurements, cytotoxicity tests, and other *in vitro* tests, with the exception of tensile tests. Cylindrical rods ($\Phi$0.7 × 5 mm) were machined parallel to the rolling direction for *in vivo* tests. All samples were mechanically polished to 2,000 grit, then ultrasonically cleaned in acetone, absolute ethanol and distilled water, before drying in open air. Polished specimens were etched in a 2% nitric acid alcohol solution and rinsed in distilled water. Afterwards, they were observed under an optical microscope (BX51M, Olympus, Japan). An X-ray diffractometer (XRD, Rigaku DMAX 2400, Japan) was adopted to identify the phase compositions by using Cu Kα radiation at a scan rate of 4° $min^{-1}$.

### Mechanical tests

The samples with a gauge length of 25 mm were processed according to ASTM-E8-04a [23]. The tensile tests were carried out on a universal material testing machine (Instron 5969, US) at a strain rate of 1 mm $min^{-1}$ at room temperature (RT). Three parallel samples were taken for each group.

### Electrochemical measurements

Electrochemical evaluation was performed with an electrochemical workstation (Autolab, Metrohm). The electrochemical measurements were performed in Hank's solution, as previously described [24]. Each sample was exposed to open-circuit potential (OCP) for 4,800 s; then potentiodynamic polarization was performed at a scanning rate of 1 mV $s^{-1}$. Corrosion potential ($E_{corr}$), corrosion current density ($i_{corr}$), and OCP were obtained by Tafel analysis based on the polarization plots. Since the determination of the Tafel slope might result in large variations [25], the Tafel slopes were carefully determined in the 130 to 300 mV potential range, away from $E_{corr}$ both on the cathodic and the anodic curves. Three duplicate samples were taken for each group.

### Immersion tests and hydrogen evolution tests

Immersion tests were performed according to ASTM G31-72 [26]. Samples were weighed prior to immersion tests with an analytical balance (METTLER TOLEDO XS105, Switzerland). At least three specimens were immersed in Hank's solution at 37°C, with the ratio of solution volume to sample surface area ($V/S$) being 20 mL $cm^{-2}$. The pH value and the volume of hydrogen evolved were recorded. Hydrogen evolution tests were carried out using a set-up described in previous study [27]. After 20 d immersion, the samples were removed from the solution, lightly rinsed with distilled water, and then dried in open air. Surface morphologies were observed with a scanning electron microscope (SEM, S-4800, Hitachi, Japan) coupled with energy dispersive spectrometer (EDS), operating in the second electron

  

mode and the backscattering electron mode. Subsequently, corrosion products were removed from the sample using chromic acid (200 g $L^{-1}$), with subsequent rinsing with distilled water, then dried in open air, before being weighed by an analytical balance.

### *In vitro* cytotoxicity test

In order to evaluate the cytotoxicity of the Mg-Li-Ca alloys, cytotoxicity tests, based on the international standard ISO 10993-5, were performed as previously described [28]. Mg-Li-Ca alloy extracts were prepared by using α-MEM supplemented with 10% fetal bovine serum (FBS) for 24 h with an extraction ratio of 1 $cm^2$ $mL^{-1}$, under cell culture conditions. Extracts ion concentrations and pH values were measured by inductively coupled plasma optical emission spectrometry (ICP-OES, iCAP6300, Thermo) and pH meter (PB-10, Sartorius), respectively.

Human bone marrow mesenchymal stem cells (hBMMSCs, Sciencell, San Diego, CA, US) were cultured in α-minimal essential medium (α-MEM, Gibco, Grand Island, NY, US) supplemented with 10% FBS, 100 U $mL^{-1}$ penicillin G, and 100 mg $mL^{-1}$ streptomycin at 37°C in an 95% air, 5% $CO_2$, in a 100% relative humidity incubator. Cells from passages 4–6 were used for *in vitro* experiments and culture medium was changed every two days. All cell related experiments were repeated no less than three times. The as-extruded pure Mg extracts and titanium (Ti) extracts were used as the material controls; culture medium was used as the negative control.

The hBMMSCs were seeded at a density of $5 \times 10^3$ cells per 100 μL medium in a 96-well plate. After 24 h cell culture, the medium was discarded and replaced with alloys extracts (experimental group) for 1, 3, and 5 d. A cell counting kit-8 (CCK8, Dojindo Laboratories, Kumamoto, Japan) was used, according to the manufacturer's protocol, to assess cell viability. Briefly, a total of 10 μL CCK8 solution was added to each well and the plate was restored to the cell incubator for 2 h. The spectrophotometric absorbance of each well was detected at a wavelength of 450 nm using a microplate reader (Elx800, Bio-Tek, Vermont, US). Each experiment was performed at least three times.

### Quantification of ALP activity

To determine the early differentiation of hBMMSCs stimulated by the extracts from Mg-Li-Ca alloys, the hBMMSCs were seeded in 12-well plates at a density of $10^4$ cells/mL in the presence of the Mg-Li-Ca alloy extracts. On day 7, the cells were rinsed with ice-cold phosphate-buffered saline (PBS) three times and then lysed with 1% triton X-100 (Sigma, St. louis, MO, US) for 10 min on ice. Cells were collected with a cell scraper, sonicated on ice, and then centrifuged at 12,000×g for 30 min at 4°C. Supernatant protein concentrations were measured using a bicinchoninic acid assay (BCA) protein assay kit (Prod#23225; Pierce Thermo Scientific, Waltham, MA, US), according to the manufacturer's instructions. Alkaline phosphatase (ALP) activity was assayed using an ALP assay kit (A059-3; Nanjing Jiancheng Bioengineering Institute, Nanjing, China). ALP levels were normalized to the total protein content, as previously described [29].

### Quantitative reverse transcription-polymerase chain reaction analyses

hBMMSCs were seeded in 6-well plates and treated by Mg-3.5Li-0.5Ca alloy extracts for 7 and 14 d. Total cellular RNA was extracted using Trizol reagent (Invitrogen, Carlsbad, CA, US), according to the manufacturer's instructions, and then reverse-transcribed into cDNA using a reverse transcription kit (Takara, Kusatsu, Shiga, Japan). Quantitative polymerase chain reaction (qPCR) analysis was performed using the SYBR Green PCR Master Mix (Roche Applied Science, Mannheim, Germany) on a 7500 sequence real-time PCR detection system (Applied Biosystems, Foster City, CA, US). The expression of glyceraldehyde 3-phosphate dehydrogenase (GADPH) was used as a housekeeping gene. Primers (Table 2) were designed based on a cDNA sequence from the National Center for Biotechnology Information (NCBI) sequence database and the primer specificity was confirmed by a BLASTN search. Cycle threshold values were used to count the fold change by using the ΔΔCt method [30].

### *In vivo* animal implantation surgery

Our research was approved by the Ethics Committee, Peking University Health Science Center, Beijing, China (PKUSSIRB-2013023). The animal experiments were conducted following the protocol established by the Experimental Animal Ethics Branch. To minimize potential suffering, all animals were anesthetized by pentobarbital sodium (50 mg $kg^{-1}$). Forty ten-week old female C57BL/6 mice were randomized into four groups ($n$ = 10): (1) Mg-3.5Li-0.5Ca alloy rods, (2) pure Mg rods, (3) titanium alloy rods, and (4) empty control group. All rods were implanted into a drilled bone tunnel in the femur along the axis of the shaft from the distal femur. In the empty control group, the drilled bone tunnel was left empty. Postoperatively, all mice were housed in an environmentally controlled animal care house.

  

**Table 2** Primer pairs used in qPCR analysis

| Gene | Forward primer | Reverse primer |
|---|---|---|
| ALP | 5'- ATGGGATGGGTGTCTCCACA-3' | 3'- CCACGAAGGGGAACTTGTC-5' |
| Runx2 | 5'-ACTACCAGCCACCGAGACCA-3' | 3'-ACTGCTTGCAGCCTTAAATGACTCT-5' |
| OCN | 5'-AGCCACCGAGACACCATGAGA-3' | 3'- GGCTGCACCTTTGCTGGACT-5' |
| OSX | 5'- ACTGCCCCACCCCTTAGACA-3' | 3'- GAGGTGCACCCCCAAACCAA-5' |
| TCF-1 | 5'- GCCATGGTTTCTAAACTGAGCCA-3' | 3'-CTTTGCTCAGCCCTGACTCG-5' |
| LEF-1 | 5'- CCTCTTGGCTGGCAAGGTCA-3' | 3'-TTGCCTGAATCCACCCGTGA-5' |
| AXIN2 | 5'- CCCCAAAGCAGCGGTGC-3' | 3'-GCGTGGACACCTGCCAG-5' |
| GAPDH | 5'- AAGGTCGGAGTCAACGGATTTG-3' | 3'- TCCTGGAAGATGGTGATGGGAT-5' |

**Soft X-ray detection, micro-computed tomography (Micro-CT) scanning, and histological analysis**

Mice were sacrificed 2 and 8 weeks post-surgery. The femora were harvested and fixed in 10% neutral buffered formalin for 24 h at RT.

To evaluate if Mg-3.5Li-0.5Ca alloys could enhance bone formation *in vivo*, soft X-ray pictures were captured using a Senographe essential X-ray apparatus (GE, Fairfield, CT, US) under 25.0 kV, 22.5 mA, 21.0 cm conditions. Micro-CT scans were performed using a high resolution Inveon apparatus (Siemens, Munich, Germany). The scanning parameters were set at an X-ray voltage of 60 kV, anode current of 220 μA, and exposure time of 1,500 ms, for each of the 360 rotational steps. Images were acquired at an effective pixel size of 8.82 μm.

After Micro-CT analysis, the femora were dehydrated with gradient dehydration from 75% to absolute ethanol and then embedded in polymethylmetacrylate (PMMA). Subsequently, the embedded specimens were sectioned into 150 μm thick sections using a Leica SP1600 saw microtome (Leica, Hamburg, Germany) parallel to the long axis of the femoral shaft. The sections were ground and polished to 40–60 μm, followed by staining with toluidine blue for histological examination. The rest of femora were decalcified in 10% EDTA solution (pH 7.4) under constant agitation at RT for 14 d (fresh 10% EDTA solution was exchanged every 48 h). Then, the femora were embedded in paraffin and sliced into 5 μm-thick serial sections, followed by hematoxylin-eosin (HE) staining for histological examination. After HE staining, the sections were observed and images were obtained using an optical microscope (BX51, Olympus, Japan).

**Western blotting analysis and immunofluorescence staining of β-catenin protein expression**

After being treated with Mg-3.5Li-0.5Ca alloy extracts for 48 h, hBMMSCs were washed with cold PBS and lysed in radioimmunoprecipitation assay (RIPA) buffer to obtain total cell protein. For cytosolic and nuclear fractions, cells were suspended in buffer A (10 mmol $L^{-1}$ Hepes, 10 mmol $L^{-1}$ KCl, 0.1 mmol $L^{-1}$ EDTA, 0.1 mmol $L^{-1}$ EGTA, 1 mmol $L^{-1}$ DTT, 0.15% NP-40 and 1% cocktail) on ice for 10 min, centrifuged at 12,000 g for 30 s, then the cytoplasmic supernatant was collected. The remaining pellet was washed with PBS and resuspended in buffer B (20 mmol $L^{-1}$ Hepes, 400 mmol $L^{-1}$ NaCl, 1 mmol $L^{-1}$ EDTA, 1 mmol $L^{-1}$ EGTA, 1 mmol $L^{-1}$ DTT, 0.5% NP-40 and 1% cocktail), rocked for 15 min at 4°C, and then centrifuged at 14,000 rpm for 15 min before the nuclear protein supernatant was collected. The protein concentrations were measured using a BCA protein assay kit (Thermo Scientific). Briefly, loading buffer was added to the protein samples and boiled for 5 min at 99°C to achieve albumen denaturation and depolymerization. Sodium dodecyl sulfate-polyacrylamide gel electrophoresis (7.5%; SDS-PAGE) was applied to the separate protein samples and the proteins were transferred to polyvinylidene fluoride membranes (Millipore). The membranes were blocked with 5% non-fat milk for 2 h at RT and incubated with primary rabbit monoclonal antibodies specific to β-catenin (diluted 1:5000; Abcam, Cambridge, UK) overnight at 4°C, followed by incubation with secondary antibodies for 1 h at RT. The results were visualized using an ECL chemiluminescence detection system (CWBIO, Beijing, China).

hBMMSCs were washed three times in PBS and fixed with 4% paraformaldehyde for 15 min at RT. Subsequently, permeabilization with 0.25% Triton X-100 for 10 min at RT. The cells were washed another three times with PBS and blocked in 0.8% BSA-PBS for 1 h. The cells were then incubated with β-catenin primary antibodies (diluted 1:100; Abcam, Cambridge, MA, US) overnight at 4°C. These cells were then rinsed and further incubated with secondary antibodies for 1 h at RT. Finally, cell nuclei were stained with DAPI for 10 min at RT. Specimens were observed under a Confocal Zeiss Axiovert 650

  

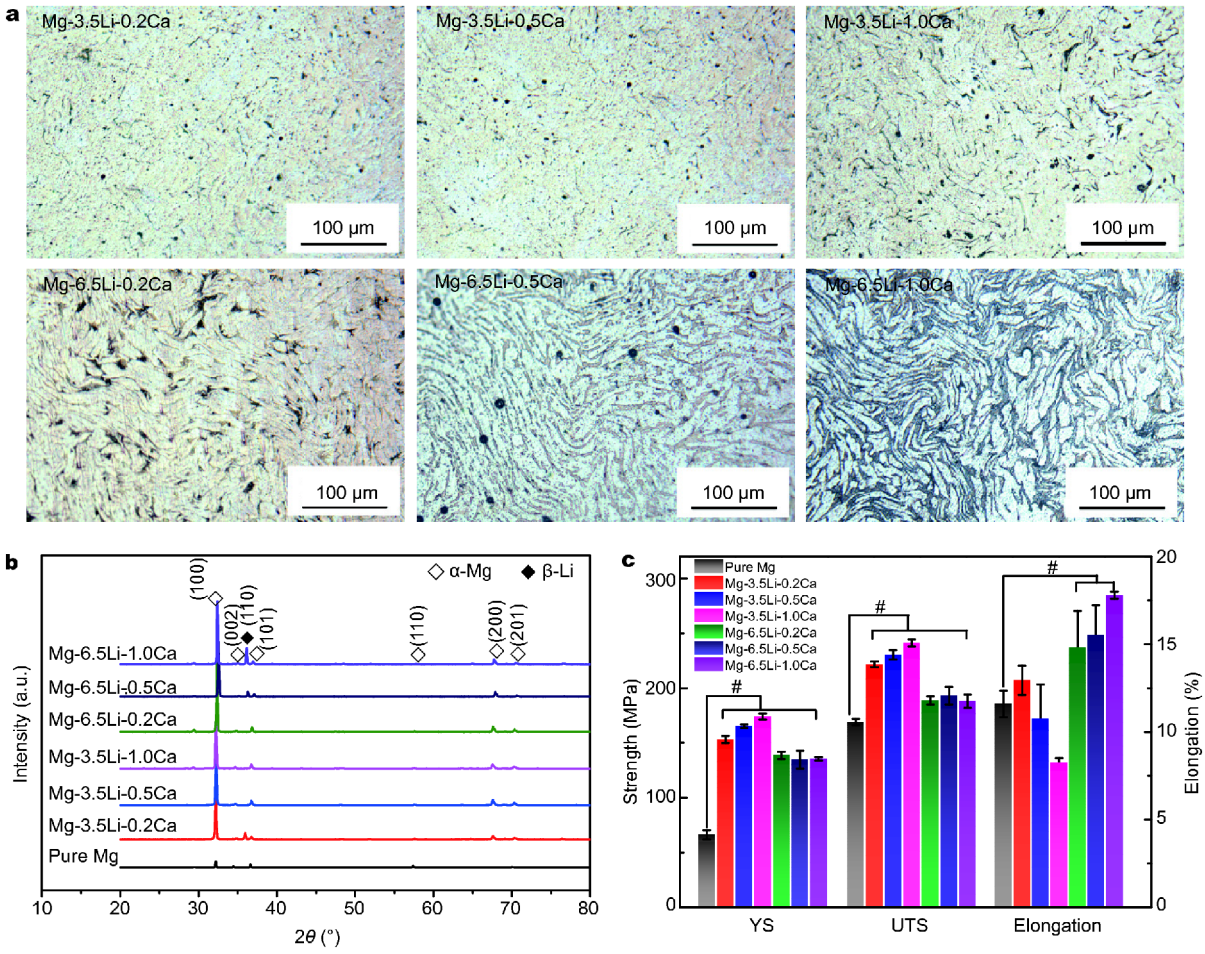


**Figure 1** Microstructures and mechanical properties of Mg-Li-Ca alloys. (a) The optical images of the cross-section perpendicular to the extrusion direction. (b) XRD results. (c) Tensile yield strength (YS), ultimate tensile strength (UTS), and elongation values of the as-extruded Mg-Li-Ca alloys. $^{\#}p<0.05$.

microscope (Carl Zeiss Microimaging, LLC, Thornwood, NY, US) under excitation wavelengths of 488 nm (green, β-catenin) and 405 nm (blue, DAPI). Statistical analysis

Data are presented as the mean value ± standard deviation and analyzed using SPSS version 16.0 (SPSS Inc., Chicago, IL, US). One-way analysis of variance (ANOVA) was performed for data analysis. Statistically significance was defined as $p$ value of $< 0.05$.

## RESULTS

### Microstructures and mechanical properties

Fig. 1a shows the optical microstructure of an as-extruded Mg-Li-Ca alloy from a cross-section perpendicular to the extrusion direction. The Mg-3.5Li-$x$Ca alloys performed a single phase with Ca-contained precipitations, which became continuous when the Ca content reached 1.0 wt%. When the Li component was 6.5 wt%, the Mg-6.5Li-$x$Ca alloys exhibited typical α-Mg + β-Li dual phase microstructure, which is similar to that of Mg-6.5Li-$x$Zn alloys reported in a previous study [24]. However, no curling or Van Gogh Sky patterns were observed on the surface. According to a previous study, Ca tends to accumulate at grain boundaries, especially in the β-Li phase [22]. The microstructure was further confirmed by XRD examination (Fig. 1b), which indicated that Mg-3.5Li-$x$Ca alloys assumed the α-Mg phase and Mg-6.5Li-$x$Ca alloys assumed the α-Mg and β-Li phase. However, $Mg_2Ca$ precipitates at the grain boundaries were not detected.

The tensile properties of the Mg-Li-Ca alloys are shown in Fig. 1c. As expected, the combined addition of Li and Ca greatly improved the mechanical properties of the as-extruded Mg-Li-Ca alloys, compared to the as-extruded Mg counterparts. The yield strength (YS) of all the Mg-

  

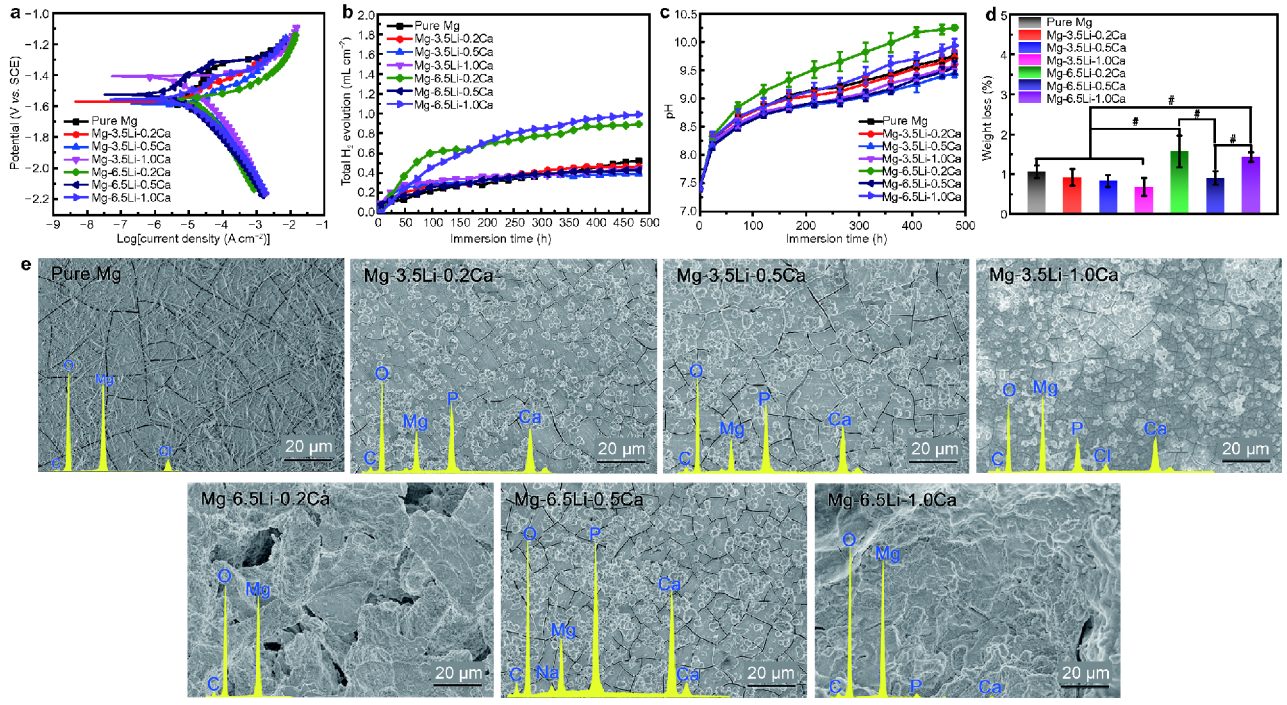


**Figure 2** Biodegradation behavior of Mg-Li-Ca alloys. (a) Potentiodynamic polarization, (b) total hydrogen evolution. (c) pH of Hank's solution. (d) Weight loss of Mg-Li-Ca alloys. $^{\#}p<0.05$. (e) Surface morphologies detected after 20 d immersion in Hank's solution.

**Table 3** Open circuit potential, corrosion potential ($E_{corr}$), corrosion current density ($I_{corr}$) and corrosion rate values obtained from the electrochemical tests

| | Open circuit potential ($V_{SCE}$) | $E_{corr}$ ($V_{SCE}$) | $I_{corr}$ (μA cm$^{-2}$) | Corrosion rate (mm y$^{-1}$) |
|---|---|---|---|---|
| Pure Mg | −1.66 ± 0.01 | −1.57 ± 0.02 | 9.3 ± 0.6 | 0.21 ± 0.01 |
| Mg-3.5Li-0.2Ca | −1.67 ± 0.03 | −1.57 ± 0.01 | 19.0 ± 4.0 | 0.40 ± 0.10 |
| Mg-3.5Li-0.5Ca | −1.66 ± 0.01 | −1.58 ± 0.02 | 21.0 ± 8.0 | 0.50 ± 0.20 |
| Mg-3.5Li-1.0Ca | −1.58 ± 0.01 | −1.45 ± 0.01 | 16.0 ± 4.0 | 0.38 ± 0.09 |
| Mg-6.5Li-0.2Ca | −1.63 ± 0.02 | −1.55 ± 0.01 | 24.0 ± 3.0 | 0.54 ± 0.07 |
| Mg-6.5Li-0.5Ca | −1.68 ± 0.02 | −1.56 ± 0.01 | 17.0 ± 12.0 | 0.40 ± 0.30 |
| Mg-6.5Li-1.0Ca | −1.67 ± 0.03 | −1.56 ± 0.05 | 21.0 ± 10.0 | 0.50 ± 0.20 |

Li-Ca alloys was at least double that of pure Mg. Single α phase based Mg-3.5Li-*x*Ca alloys exhibited higher YS than dual phase Mg-6.5Li-*x*Ca alloys. Moreover, incorporation of the Ca component was efficient in terms of alloy strengthening, with monotone increasing YS and ultimate tensile strength (UTS) with increasing Ca content from 0.2 to 1.0 wt% in the Mg-3.5Li-*x*Ca alloys. Specifically, the UTS of Mg-3.5Li-1.0Ca and Mg-3.5Li-0.5Ca were, respectively, 241 ± 3 and 230 ± 4 MPa, which were significantly higher than that of pure Mg (169 ± 3 MPa). Meanwhile, the as-extruded Mg-6.5Li-*x*Ca exhibited significantly improved elongation.

### Corrosion behavior

*In vitro* corrosion tests, including electrochemical, immersion, and hydrogen evolution analyses, as well as the calculated electrochemical corrosion results, are detailed in Fig. 2 and Table 3. The corrosion current density results illustrate the transient behavior of the metals with time. Interestingly, after the addition of Li and Ca, all of the as-extruded Mg-Li-Ca alloy OCP and $E_{corr}$ values were not significantly different than the as-extruded pure Mg. Meanwhile, the corrosion rates were significantly higher. Potentiodynamic polarization analysis was conducted about two hours after the sample surfaces were exposed

  

to the Hank's solution, since OCP test was conducted before it. All the Mg-Li-Ca samples exhibited increased corrosion current densities and, therefore, increased corrosion abilities compared to the as-extruded pure Mg. These results highlight the as-extruded Mg-Li-Ca alloy reactivity in Hank's solution over the initial few hours.

However, the 20 d immersion tests demonstrate a quite different corrosion trend during long time static immersion. In terms of hydrogen evolution (Fig. 2b), both the as-extruded Mg-6.5Li-0.2Ca and Mg-6.5Li-1.0Ca alloy samples released a lot more hydrogen than pure Mg or other Mg-Li-Ca groups, although in the first 50 h they did not show such trend. The hydrogen quantities released from the as-extruded Mg-3.5Li-0.2Ca, Mg-3.5Li-0.5Ca, Mg-3.5Li-1.0Ca, and Mg-6.5Li-0.5Ca samples are comparable to that from the as-extruded pure Mg. They even showed less hydrogen release at 20 d than the as-extruded pure Mg. Meanwhile, the pH monitoring supported these results, as shown in Fig. 2c. The as-extruded Mg-6.5Li-0.2Ca and Mg-6.5Li-1.0Ca alloy samples resulted in higher pH values than the as-extruded pure Mg in Hank's solution, whilst the other four as-extruded Mg-Li-Ca alloys resulted in lower pH values than the as-extruded pure Mg. The 20 d weight loss results also corroborated these results, as shown in Fig. 2d. The surface morphologies of the as-extruded Mg-Li-Ca alloys and pure Mg, used as the control, are shown in Fig. 2e. The as-extruded pure Mg underwent local corrosion, with some parts on its surface exhibiting few signs of corrosion, with other parts exhibiting severe surface corrosion with heavy product aggregation. Therefore, we chose the moderately corroded sections to qualitatively represent the corrosion performance of these samples. As shown, needle-shaped corrosion products were observed on the surface of the as-extruded pure Mg, which was reported to be $Mg(OH)_2$ [31]. As for the as-extruded Mg-6.5Li-0.2Ca and Mg-6.5Li-1.0Ca alloy samples, both clearly underwent severe corrosion over the 20 d immersion and barely maintained their surface integrity. The surfaces were severely damaged and lost their planar appearance, with $Cl^-$ and other corrosive ions penetrating inside the samples. Additionally, the EDS results confirmed little Ca/P could aggregate on the surfaces due to highly-active corrosion. In comparison, the as-extruded Mg-3.5Li-0.2Ca, Mg-3.5Li-0.5Ca, Mg-3.5Li-1.0Ca, and Mg-6.5Li-0.5Ca alloy samples all maintained their planar surface form with Ca/P corrosion product deposition. Interestingly, *in vitro* corrosion measurements, including electrochemical and immersion tests, revealed that the as-extruded Mg-Li-Ca alloys exhibited higher corrosion trends in the first few hours of immersion, but better corrosion resistance with longer term immersion.

### Cell cytotoxicity and ALP activity

To compare the proliferation of hBMMSCs cultured in the presence of the alloy extracts, CCK8 assays were performed. As shown in Fig. 3a, none of the alloy extracts were toxic to hBMMSCs after 1, 3, and 5 d of incubation. On 3 and 5 d of culture, the highest cell proliferation was observed for cells cultured in the presence of Mg-3.5Li-0.5Ca alloy extracts. Cytoskeleton staining data of hBMMSCs were shown in Supplementary information, Fig. S1. Cells cultured in Mg-Li-Ca alloy extracts had good spreading morphologies and visible stained cytoplasmic filament. ALP activity, which is considered an early osteogenic differentiation marker, was examined. Quantitative analysis revealed that the ALP activity of hBMMSCs cultured in the presence of Mg-3.5Li-0.5Ca alloy extracts was higher than other groups on day 7 (Fig. 3b). The Mg-3.5Li-0.5Ca alloy exhibited the highest ability to promote osteogenic differentiation in hBMMSCs.

Alloy extracts pH and ion concentration values are shown in Fig. 3c and d. The pH values in the various extracts ranged from 8.43 to 8.81. $Mg^{2+}$ ion concentrations in the various extracts ranged from 106.4 to 130.2 μg $mL^{-1}$, $Li^+$ ion concentrations fluctuated between 5.1 and 13.3 μg $mL^{-1}$, while $Ca^{2+}$ ion concentrations ranged from 56.1 to 59.5 μg $mL^{-1}$.

### Osteogenic differentiation of hBMMSCs in the presence of Mg-3.5Li-0.5Ca alloy extracts

To further investigate the influence of Mg-3.5Li-0.5Ca alloy extracts on the osteogenic differentiation of hBMMSCs, the expression levels of osteogenesis related genes Runx2, ALP, OCN, and OSX were examined by qPCR. As illustrated in Fig. 4, the expression of Runx2, ALP, OCN, and OSX was apparently up-regulated after 7 and 14 d of culture.

### *In vivo* study

All mice survived the observation period. The surgical wounds showed no visible inflammation during the study. The mice were sacrificed after 2 and 8 weeks.

Soft X-ray analyses of representative samples are shown in Fig. 5a. All implants were well positioned well within the distal femur and there were no translucent areas. Bone hyperplasia was observed around the cortical bone surrounding Mg-3.5Li-0.5Ca and pure Mg alloy implants after 2 weeks. In the titanium and blank control group, no

  

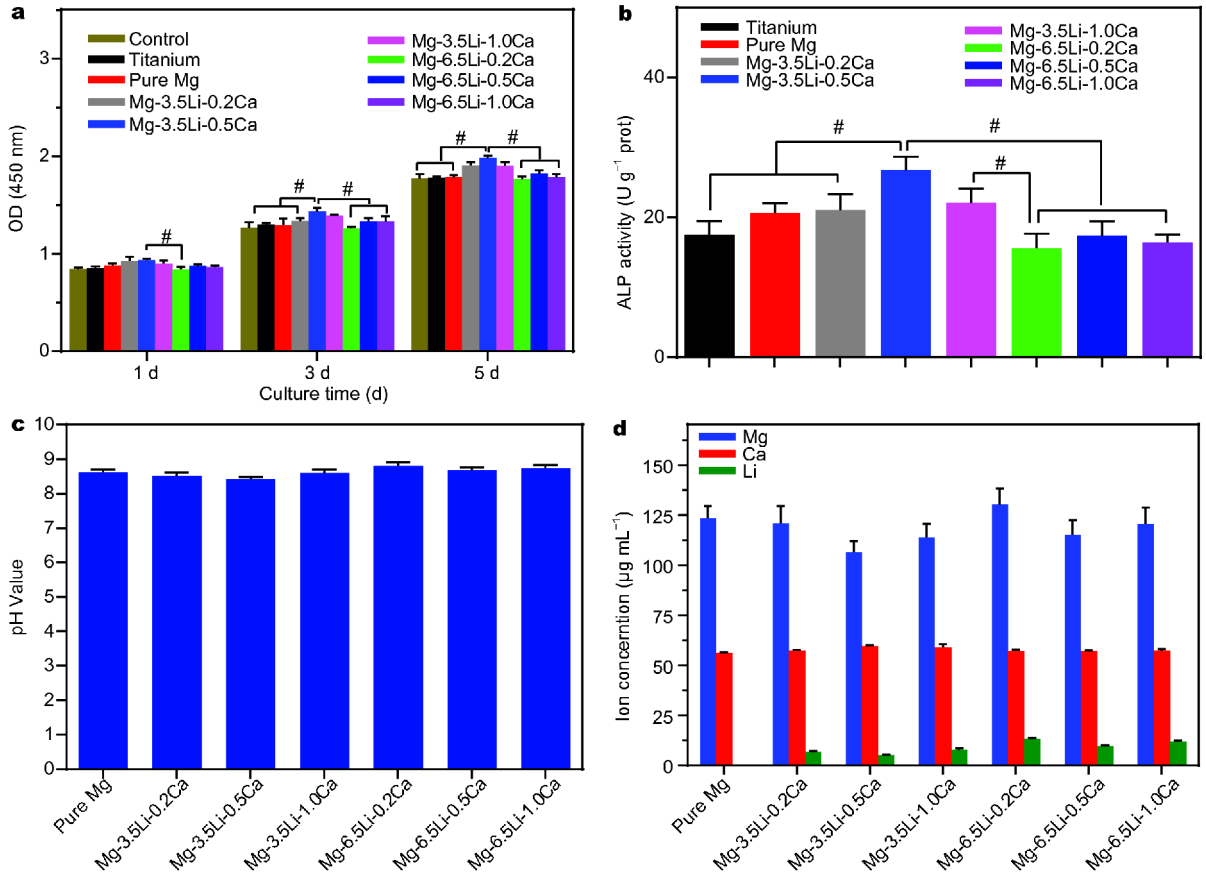


**Figure 3** Cell cytotoxicity and ALP activity of Mg-Li-Ca alloys. (a) OD value of hBMMSCs cultured in alloy extracts. $^{\#}p<0.05$. (b) ALP activity to Mg-Li-Ca alloy extracts. $^{\#}p<0.05$. (c) pH values of the alloy extracts. (d) Ion concentrations of the alloy extracts.

bone hyperplasia was observed. After 8 weeks, the cortical bone was thicker in the Mg-3.5Li-0.5Ca alloy and pure Mg alloy groups than the titanium and blank control group. Micro-CT reconstruction of the distal femur illustrated that the cortical bone thickness around the Mg-3.5Li-0.5Ca alloy rods and pure Mg was higher than in the titanium and blank control groups (Fig. 5c). No significant differences were found between the Mg-3.5Li-0.5Ca alloy and pure Mg alloy groups. The densities of the Mg-3.5Li-0.5Ca alloy and pure Mg implants decreased gradually over the observation period.

Analysis of distal femora longitudinal hard tissue slices stained with toluidine blue clearly shows that the bone thickness around the implanted Mg-3.5Li-0.5Ca alloy rods and pure Mg alloy rods was higher than that of the titanium rod and the empty group (Fig. 5d), which is consistent with the soft X-ray and Micro-CT results. The Mg-3.5Li-0.5Ca alloy rods and pure Mg alloy rods degraded and the degradation products diffused into the bone marrow cavity; the magnified picture shows the new bone formation clearly and a higher quantity of bone trabeculae could be observed in the Mg-3.5Li-0.5Ca alloy group and pure Mg alloy rod group than the titanium group and the blank control group. HE staining supported the toluidine blue results (Fig. 5e). No polymorphonuclear cells or foreign body giant cells were observed.

Optical images of the HE stained sections of organs were displayed in Fig. S2. The heart, kidney, liver and spleen obtained from the Mg-3.5Li-0.5Ca alloy group showed similar cell structures compared with the control group. Serum $Li^+$ concentration of mice after 2 and 8 weeks are shown in Fig. S3. No significant differences were found between the Mg-3.5Li-0.5Ca alloy and the control groups.

### Mg-3.5Li-0.5Ca alloys promote osteogenic differentiation by activation of the canonical Wnt/β-catenin pathway

In order to determine if the Wnt signaling pathway participated in the regulation of osteogenic differentiation

  

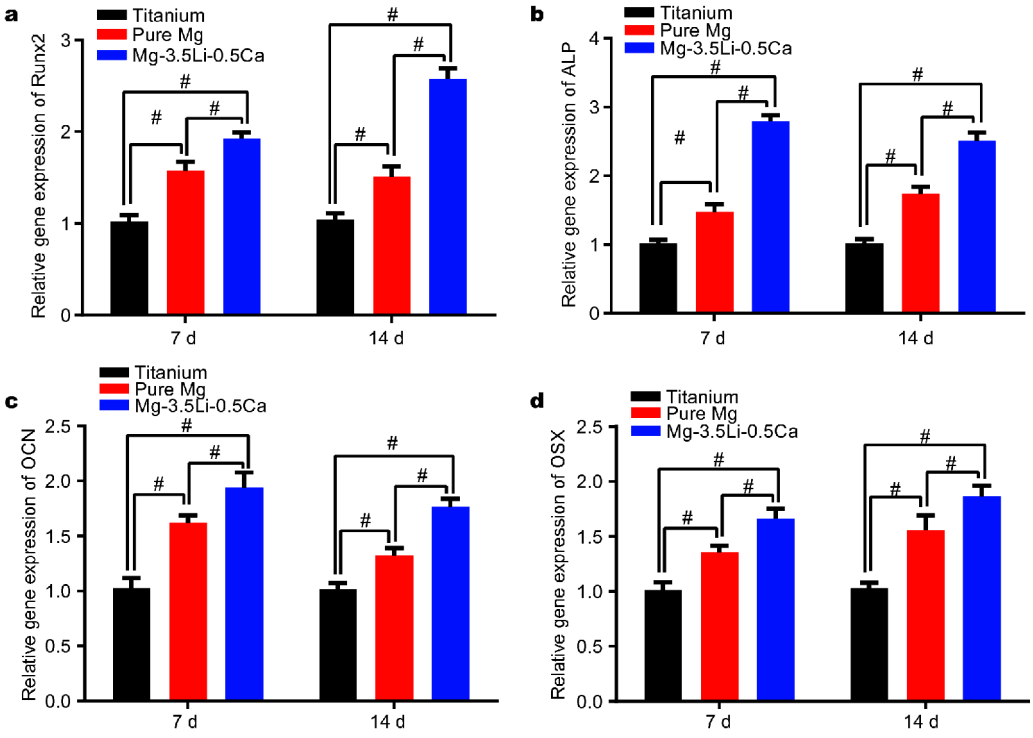


**Figure 4** Osteogenic differentiation of hBMMSCs treated by Mg-3.5Li-0.5Ca alloy extracts after 7 and 14 d. The expression of osteogenic genes Runx2 (a), ALP (b), OCN (c) and OSX (d) of hBMMSCs. $^{\#}p<0.05$.

by Mg-3.5Li-0.5Ca alloy extracts, the protein expression of key molecules in the Wnt/β-catenin pathway was analyzed using western blot analysis after 48 h of treatment with Mg-3.5Li-0.5Ca alloy extracts. As shown in Fig. 6a, the presence of Mg-3.5Li-0.5Ca alloy extracts significantly decreased GSK-3β levels, and increased the total β-catenin levels. Further data analysis revealed that the β-catenin level in the presence of Mg-3.5Li-0.5Ca alloy extracts was significantly higher than the control group (Fig. 6b). Nuclear β-catenin, which is a marker for β-catenin signaling activation, was also enhanced after 48 h of stimulation with the Mg-3.5Li-0.5Ca alloy extracts (Fig. 6c), with nuclear β-catenin levels significantly higher than in the pure Mg group (Fig. 6d). It is demonstrated by analysis of these results that β-catenin was expressed at higher levels after treatment with Mg-3.5Li-0.5Ca alloy extracts. qPCR results showed that the Wnt signal pathway-related genes LEF-1, TCF-1, and Axin2 increased in the presence of Mg-3.5Li-0.5Ca alloy extracts compared to the control group (Fig. 6e).

To confirm these findings, the expression of β-catenin was examined by immunofluorescence staining. After hBMMSCs were exposed to Mg-3.5Li-0.5Ca alloy extracts for 48 h, β-catenin presented a much stronger fluorescent signal and translocated into the nucleus (Fig. 6f). This result is consistent with the protein results and indicates that Mg-3.5Li-0.5Ca alloys play an important role in osteogenic differentiation of hBMMSCs *via* the canonical Wnt/β-catenin pathway.

## DISCUSSION

An ideal biodegradable biomaterial should exhibit biocompatibility, mechanical strength and a suitable degradation rate. In this vein, magnesium alloys are considered good candidates for bone implantation due to their favorable biodegradation and mechanical strength. In the present study, we developed Mg-3.5Li-0.5Ca alloys, with a view to implantation, which shows favorable mechanical strength and corrosion resistance *in vitro*. Moreover, we also studied the *in vivo* performance of Mg-3.5Li-0.5Ca alloys and explored their mechanism for promoting the osteogenic differentiation of hBMMSCs.

### Mechanical properties and biodegradation behavior

Upon examination of the results presented herein, it is clear that both Li and Ca strongly influence the mechanical and corrosion behavior of the alloys. Table 4 summarizes the mechanical and corrosion behavior of

  

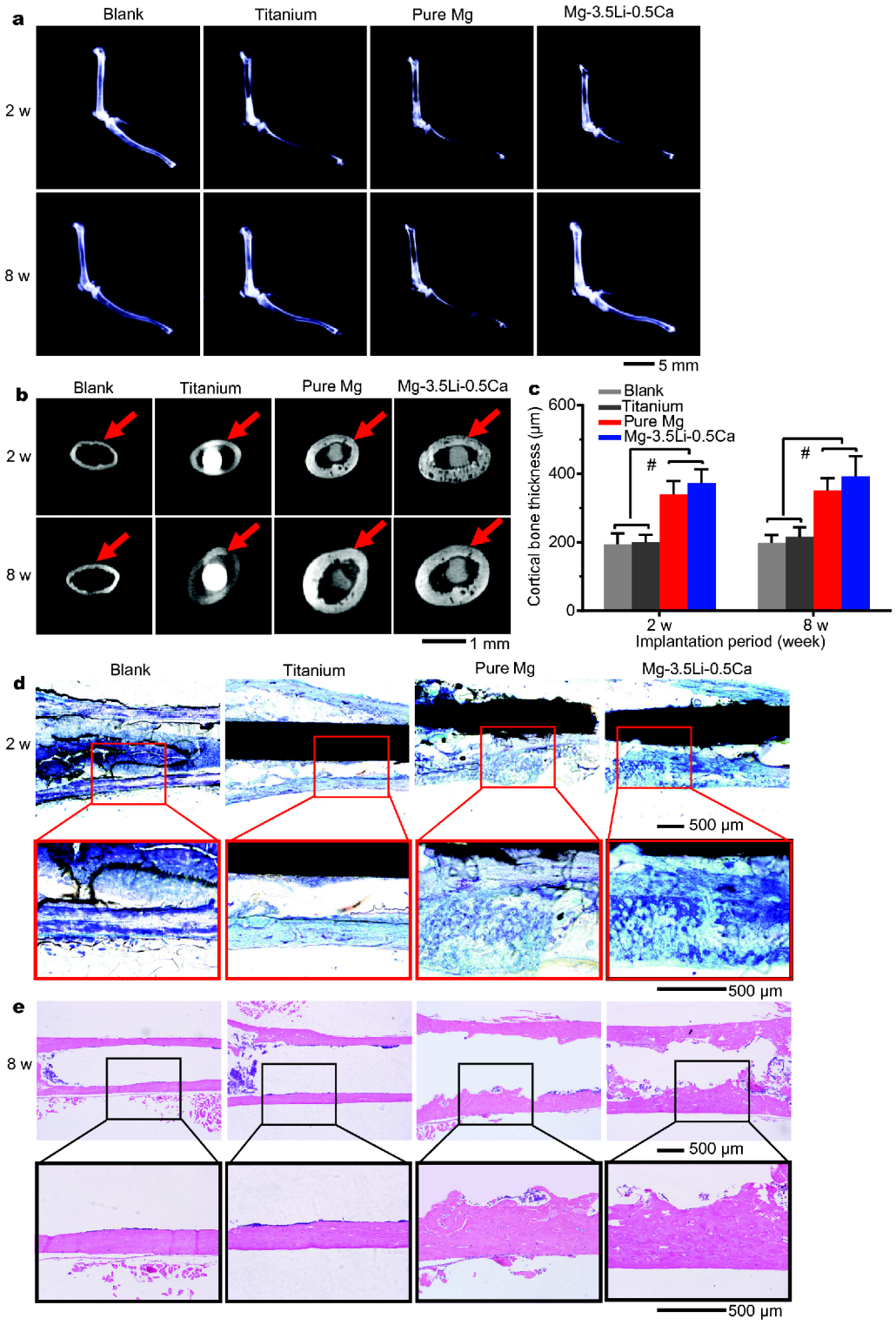


**Figure 5** *In vivo* performance of Mg-3.5Li-0.5Ca alloys. (a) The radiographs of mice femora after implantation evaluated after 2 and 8 weeks. (b) Micro-CT images of the transverse sections of canine femurs with implants 2 and 8 weeks after implantation. (c) Cortical bone thickness in all groups at different implantation intervals. $^{\#}p<0.05$. (d) Representative histological observation of the femora hard tissue section stained with toluidine blue by light microscopy. (e) Representative histological observation of the femora haematoxylin and eosin (HE) section by light microscopy.

  

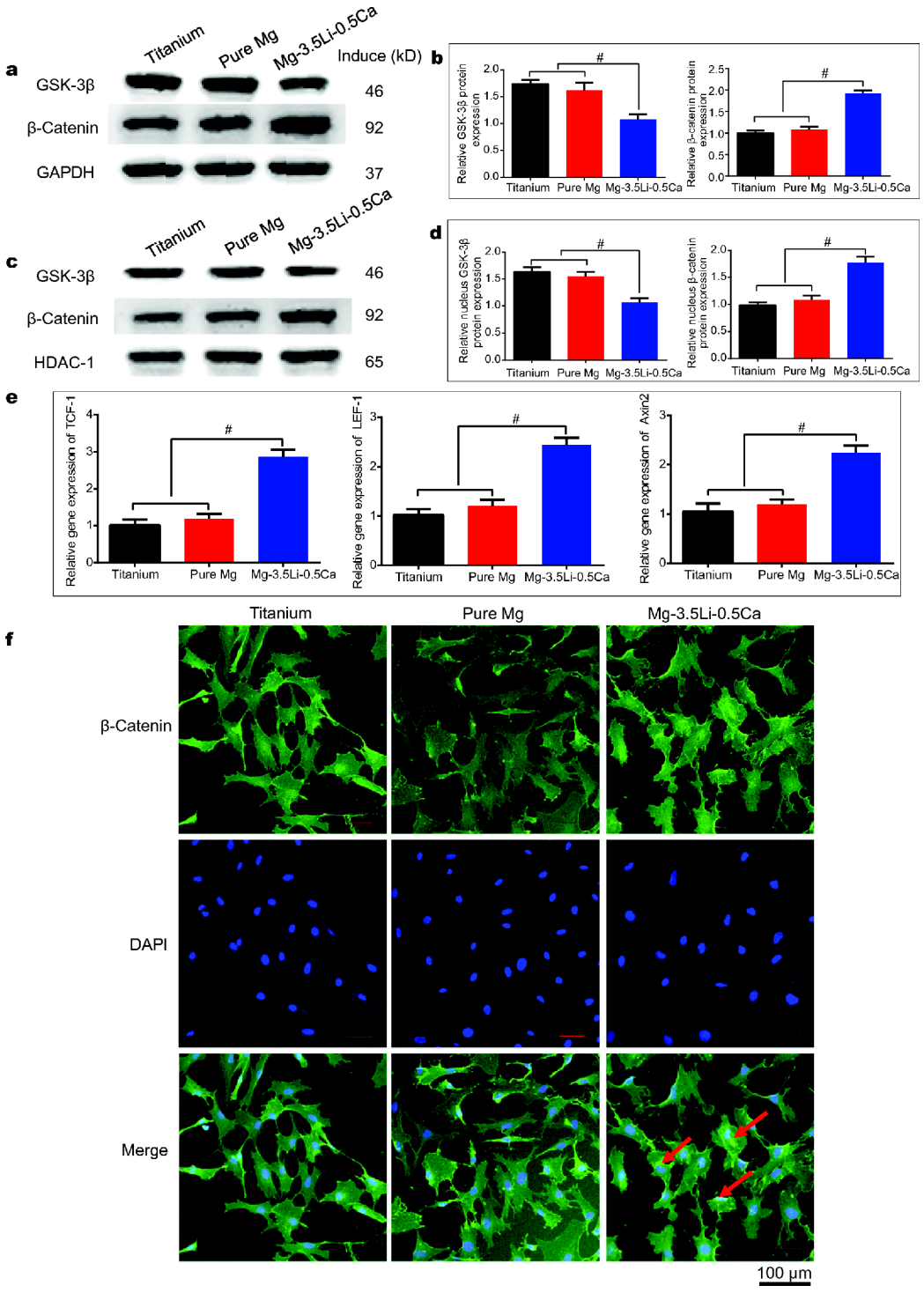


**Figure 6** Activity of canonical Wnt/β-catenin pathway stimulated by Mg-3.5Li-0.5Ca alloy. (a) Western blotting analysis illustrated increased total GSK-3β and β-catenin expression in Mg-3.5Li-0.5Ca alloy extracts after 48 h. (GAPDH was used as the internal control). (b) Quantitation of GSK-3β and β-catenin expression levels obtained from Image J. $^{\#}p<0.05$. (c) Western blotting analysis exhibited increased nucleus GSK-3β and β-catenin expression in Mg-3.5Li-0.5Ca alloy extracts after 48 h. (HDAC-1 was used as internal nucleus control). (d) Quantitation of nucleus GSK-3β and β-catenin expression levels obtained from Image J. $^{\#}p<0.05$. (e) Expression of Wnt signal pathway-related genes (LEF-1, TCF-1 and Axin2) in hBMMSCs cultured in different groups after 48 h. $^{\#}p<0.05$. (f) Intracellular localization of β-catenin visualized by immunofluorescence. β-Catenin is colored green and nuclei are colored blue.

**Table 4** Summary of the mechanical and corrosion behavior of reported Mg-Li based alloys for biomedical application

| Composition | Mechanical behavior | | | Corrosion behavior | | Ref. |
|---|---|---|---|---|---|---|
| | YS (MPa) | UTS (MPa) | Elongation (%) | Corrosion rate (mm $y^{-1}$, electrochemical) | Weight loss (Hank's solution) | |
| Pure Mg | 66 ± 4 | 169 ± 3 | 11.6 ± 0.7 | 0.21 ± 0.01 | (1.1 ± 0.2)% | |
| Mg-9.29Li-0.88Ca | 107 .8 | 113.4 | 52.8 | 2.81 ± 0.22 | 1.38 ± 0.16 mm $y^{-1}$ | [22] |
| Mg-3.5Li | ~75 | ~150 | ~15 | 0.1 | \ | |
| Mg-8.5Li | ~75 | ~100 | ~42 | 0.16 | \ | |
| Mg-3.5Li-1Al | ~90 | ~150 | ~46 | 0.1 | \ | [32] |
| Mg-3.5Li-2Al-2RE | ~90 | ~190 | ~22 | 0.34 | \ | |
| Mg-3.5Li-4Al-2RE | ~140 | ~230 | ~23 | 0.24 | \ | |
| Mg-8.5Li-2Al-2RE | ~100 | ~150 | ~32 | 0.16 | \ | |
| Mg-3.5Li-0.5Zn | 130 ± 5 | 203 ± 4 | 20 ± 2 | 0.34 ± 0.03 | \ | |
| Mg-3.5Li-2Zn | 165 ± 3 | 246 ± 2 | 22 ± 2 | 0.24 ± 0.01 | \ | |
| Mg-3.5Li-4Zn | 163 ± 6 | 250 ± 10 | 22 ± 3 | 0.32 ± 0.04 | \ | |
| Mg-6.5Li-0.5Zn | 153 ± 5 | 223 ± 6 | 23 ± 1 | 0.34 ± 0.07 | \ | [24] |
| Mg-6.5Li-2Zn | 141 ± 1 | 190 ± 3 | 35 ± 1 | 0.30 ± 0.01 | \ | |
| Mg-6.5Li-4Zn | 167 ± 3 | 231 ± 4 | 29 ± 2 | 0.28 ± 0.02 | \ | |
| Mg-1Li-1Ca | ~130 | ~180 | ~10 | 1.48 | \ | |
| Mg-9Li-1Ca | ~80 | ~115 | ~53 | 2.92 | \ | [33] |
| Mg-15Li-1Ca | ~80 | ~115 | ~25 | 6.26 | \ | |
| Mg-3.5Li-0.2Ca | 153 ± 3 | 221 ± 2 | 13 ± 1 | 0.4 ± 0.1 | (0.9 ± 0.2)% | |
| Mg-3.5Li-0.5Ca | 165 ± 2 | 230 ± 4 | 11 ± 2 | 0.5 ± 0.2 | (0.8 ± 0.2)% | |
| Mg-3.5Li-1.0Ca | 173 ± 3 | 241 ± 3 | 8.3 ± 0.2 | 0.38 ± 0.09 | (0.7 ± 0.2)% | The present study |
| Mg-6.5Li-0.2Ca | 139 ± 3 | 189 ± 4 | 15 ± 2 | 0.54 ± 0.07 | (1.6 ± 0.4)% | |
| Mg-6.5Li-0.5Ca | 135 ± 8 | 193 ± 8 | 16 ± 2 | 0.4 ± 0.3 | (0.9 ± 0.2)% | |
| Mg-6.5Li-1.0Ca | 135 ± 2 | 188 ± 6 | 17.8 ± 0.2 | 0.5 ± 0.2 | (1.4 ± 0.1)% | |

recently reported Mg-Li based alloys developed for biomedical applications, against pure Mg used as a comparison. The addition of Li leads to large variations in mechanical properties and elongation, which makes it possible to tailor the mechanical properties of the alloys for different target applications. It is well documented that the addition of Li influences the crystal structure of Mg-Li based alloys [34]. According to the summary, generally, the addition of Li results in less strength but higher elongation, while the addition of other alloying elements can increase strength due to solid solution strengthening and precipitation strengthening effects. In our study, we chose the most naturally abundant metallic element in the human body, Ca, with a view to improving implant mechanical performance, while minimizing adverse effects [22]. As biodegradable metals, current Mg-Li-Ca alloys especially the Mg-3.5Li-0.5Ca and Mg-3.5Li-1.0Ca show favorable degradation qualities and comparable corrosion behavior, when compared to pure Mg counterparts. Furthermore, the reported $Li_2CO_3$ protective layer provides an alternative strategy to other biodegradable Mg alloys to achieve better corrosion resistance [9,22,24].

Besides composition, the machining process contributes to the final properties of the Mg-Li-Ca alloys. The higher extrusion ratio and extrusion temperature along with higher Li addition led to much higher elongation in Mg-9.29Li-0.88Ca [22], while the lower extrusion ratio and extrusion temperature along with slight lower Li content resulted in high mechanical properties and better corrosion resistance in the present Mg-6.5Li-*x*Ca alloys.

### *In vitro* cytocompatibility of Mg-Li-Ca alloy extracts

Our results suggest that the Mg-Li-Ca alloy extracts stimulate hBMMSCs viability, when compared with the control groups (Fig. 3a). A previous study indicated that the maximum $Mg^{2+}$ ion concentration that resulted in any measurable adverse effects on BMSCs was 27.6 mmol $L^{-1}$

  

[35]; other researchers reported that less than 10 mmol $L^{-1}$ $Mg^{2+}$ ion concentration did not inhibit the viability and osteogenic differentiation of hBMMSCs [36]. These concentrations are much higher than the $Mg^{2+}$ ion concentration used in our research. $Li^{+}$ ion concentrations of less than 5 mmol $L^{-1}$ have been shown to increase hBMMSCs proliferation [37]. The $Li^{+}$ ion concentrations in our extracts were below 2 mmol $L^{-1}$. The effect of $Ca^{2+}$ ion concentration on cell behavior was not studied, as the $Ca^{2+}$ ion concentration in cell culture medium was not increased. The pH values in our extracts ranged from 8.43 to 8.81 (Fig. 3c). It has been reported that suitable pH conditions for cell viability and proliferation should be near to neutral [38]. However, previous studies have shown that an alkaline pH had no adverse effects on human embryonic stem cell proliferation and BMSCs [35,39]. This disparity may be attributed to the varying sensitivity of different cell types; thus, hBMMSCs may tolerate increased pH conditions in the Mg-Li-Ca alloy extracts. This is in accordance with previous reports that an alkaline environment stimulated cell growth in BMSCs [40]. The current *in vitro* study shows the alloy's suitable biocompatibility.

### *In vivo* animal implantation study

To our knowledge, this is the first study to examine the *in vivo* performance of Mg-3.5Li-0.5Ca alloys. The soft X-ray and Micro-CT results demonstrate that the Mg-3.5Li-0.5Ca and pure Mg alloy enhanced cortical bone thickness in comparison to the titanium alloy and blank controls. This may be due to released $Mg^{2+}$ ions, which are a by-product of the Mg-3.5Li-0.5Ca alloy and pure Mg. Previous studies have shown that $Mg^{2+}$ ions are crucial to promote bone formation [1,41,42]. Moreover, $Li^{+}$ ions released from the Mg-3.5Li-0.5Ca alloys may promote bone formation. Several reports have shown that $Li^{+}$ ions can enhance the osteogenic differentiation of BMSCs [43,44]. As shown in Fig. 5, both the Mg-3.5Li-0.5Ca alloy and pure Mg exhibited bone promotion ability. However, pure Mg exhibits low mechanical strength properties. As a result, it is not suitable for load-bearing areas, due to losses in integrity and strength during degradation. Thus, the current *in vivo* study provides evidence for the superior potential of the Mg-3.5Li-0.5Ca alloy for biomedical implantation.

### Mechanism of hBMMSCs osteogenic differentiation promotion by Mg-3.5Li-0.5Ca alloy extracts

It is widely accepted that $Mg^{2+}$ is abundant in the skeleton and is essential in bone development, facilitating the mineralization and osteogenesis of MSCs [45]. Previous studies have shown that high $Mg^{2+}$ ion concentrations can lead to bone cell activation [1]. Moreover, it has been reported that $Mg^{2+}$ ions from $MgSO_4$ can stimulate the osteogenic differentiation of hBMMSCs [46]. However, few studies have focused on the influence of Mg-3.5Li-0.5Ca alloy extracts on hBMMSCs, which, of course, more closely simulates a clinical/physiological scenario. Therefore, we investigated the influence of Mg-3.5Li-0.5Ca alloy extracts on hBMSC osteogenic differentiation. Runx2 is a key transcription factor in osteogenic differentiation, which can trigger osteoblast formation and regulate osteoblast-specific gene expression, for example BSP, OCN, and OPN [47,48]. OCN is a late stage marker, which is secreted by osteoblasts during bone formation. It can modulate the growth of hydroxyapatite and regulate the metabolism of bone [49]. OSX is a master regulator of osteoblast differentiation, specifically expressed in all developing bones [50]. The results show that the expression levels of those genes were up-regulated after 7 and 14 d of culture (Fig. 4). This illustrates that the Mg-3.5Li-0.5Ca alloy extracts significantly promote osteogenic differentiation.

To the authors' knowledge, the detailed molecular mechanism through which Mg-3.5Li-0.5Ca alloy extracts promote the osteogenic differentiation of hBMMSCs has not been revealed. To further elucidate the possible mechanisms, we examined the canonical Wnt/β-catenin signaling pathway, which is believed to play a key role in osteoblast differentiation and new bone formation [51]. The Wnt/β-catenin pathway is considered to be a major modulator in osteogenesis, *via* a series of β-catenin signaling events [52].

In our study, the nucleus protein level was assessed, which is a marker for Wnt/β-catenin signaling activity [53]. Interestingly, our results indicate that Mg-3.5Li-0.5Ca alloy extracts inhibit GSK-3β activity, and consequently, GSK-3β is unable to phosphorylate β-catenin. β-catenin accumulates in the cytoplasm, translocates into the nucleus, thereby activating Wnt/β-catenin during bone formation. Additionally, the immunofluorescence staining of β-catenin also suggests that Mg-3.5Li-0.5Ca alloy extracts promote β-catenin translocation into the nucleus at an early stage (Fig. 6f). These findings suggest that the Mg-3.5Li-0.5Ca alloys promote hBMMSCs osteogenic differentiation by, at least partially, activation of the canonical Wnt/β-catenin signaling pathway.

A previous study reported that the addition of $Mg^{2+}$ ions does not activate the canonical Wnt/β-catenin pathway [54]. Meanwhile, the $Ca^{2+}$ ion concentration in

  

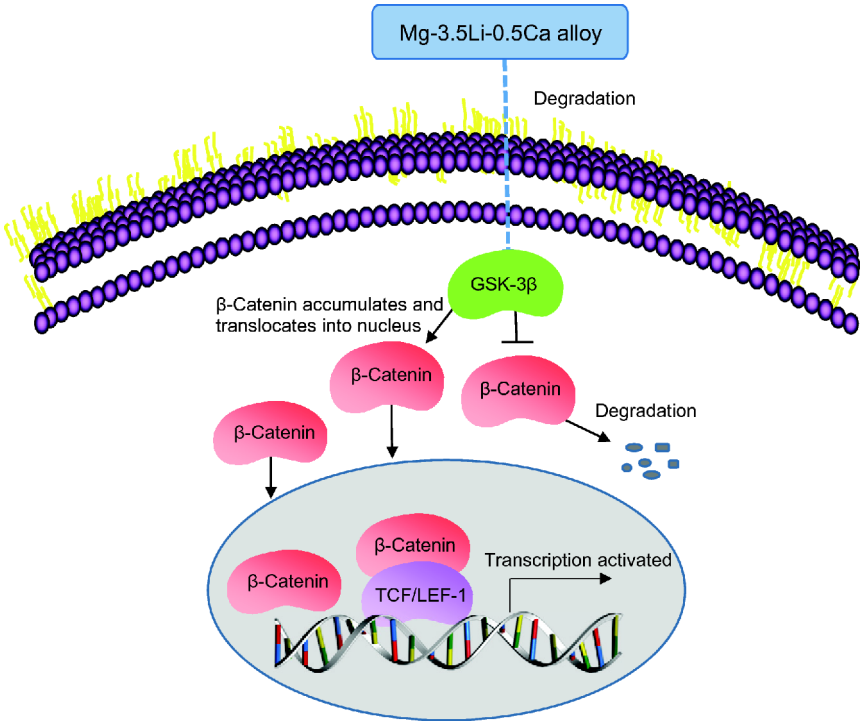


**Figure 7** Suggested mechanism of hBMMSCs osteogenic differentiation in the presence of Mg-3.5Li-0.5Ca alloys.

the presence of Mg-3.5Li-0.5Ca alloy extracts was not increased. Previous studies have shown that $Li^+$ ions could promote bone mass *in vivo* [12,14]. Researchers found that $Li^+$ doped scaffolds enhance subchondral bone regeneration through activation of the Wnt signaling pathway in BMSCs [37]. Therefore, we speculate that $Li^+$ ions released from the Mg-3.5Li-0.5Ca alloy may be the main factor in the activation of the Wnt/β-catenin signaling pathway.

Based on the above analyses, we propose a working model to account for the promotion of hBMMSCs osteogenic differentiation by Mg-3.5Li-0.5Ca alloys (Fig. 7). The canonical Wnt/β-catenin pathway is stimulated by the binding of a Wnt protein to its corresponding cell membrane receptor, thus inhibiting a complex comprised of Axin, glycogen synthase kinase 3β (GSK-3β), and adenomatous polyposis coli (APC), which degrades cytoplasmic β-catenin. Consequently, GSK-3β is unable to phosphorylate β-catenin, thus β-catenin accumulates in the cytoplasm and translocates into the nucleus to react with the transcription factor T cell factor (TCF), and then target genes are activated.

Taken together, our results demonstrate, for the first time, that Mg-3.5Li-0.5Ca alloy extracts can promote hBMMSCs osteogenic differentiation by means of improving osteogenic-specific genes and protein expressions. The activation of the canonical Wnt/β-catenin pathway seems to be the main mechanism involved in the osteogenic differentiation of hBMMSCs after exposure to Mg-3.5Li-0.5Ca alloy extracts. This should enrich our knowledge concerning the mechanisms by which bone-implant biomaterials promote osteogenesis. The *in vivo* assessment supports our *in vitro* observations, in terms of the influence of Mg-3.5Li-0.5Ca alloys in promoting osteogenic differentiation. Therefore, Mg-3.5Li-0.5Ca alloys should be considered as a promising implantation candidate for promoting bone regeneration.

However, there are some limitations to this study. Large animal models are needed to verify the validity of Mg-3.5Li-0.5Ca alloy implantations prior to clinical application. Moreover, there may be other mechanisms involved in the osteogenic differentiation of hBMMSCs. Therefore, further investigations are needed to aid the future clinical application of Mg-3.5Li-0.5Ca alloys.

## CONCLUSIONS

Mg-3.5Li-0.5Ca alloys were fabricated as potential biodegradable orthopedic biomaterials. The results positively point to their favorable mechanical properties, good corrosion resistance, excellent bone augmentation ability,

  

and fine biocompatibility. These findings suggest that Mg-3.5Li-0.5Ca alloys are promising candidates for bone implant application.

**Received 12 March 2018; accepted 3 May 2018; published online 8 June 2018**


1 Witte F, Kaese V, Haferkamp H, *et al. In vivo* corrosion of four magnesium alloys and the associated bone response. Biomaterials, 2005, 26: 3557–3563
2 Witte F, Fischer J, Nellesen J, *et al. In vitro* and *in vivo* corrosion measurements of magnesium alloys. Biomaterials, 2006, 27: 1013–1018
3 Cheng P, Han P, Zhao C, *et al.* High-purity magnesium interference screws promote fibrocartilaginous entheses regeneration in the anterior cruciate ligament reconstruction rabbit model *via* accumulation of BMP-2 and VEGF. Biomaterials, 2016, 81: 14–26
4 Zhao D, Huang S, Lu F, *et al.* Vascularized bone grafting fixed by biodegradable magnesium screw for treating osteonecrosis of the femoral head. Biomaterials, 2016, 81: 84–92
5 Staiger MP, Pietak AM, Huadmai J, *et al.* Magnesium and its alloys as orthopedic biomaterials: A review. Biomaterials, 2006, 27: 1728–1734
6 Witte F. The history of biodegradable magnesium implants: A review. Acta Biomater, 2010, 6: 1680–1692
7 Rössig C, Angrisani N, Helmecke P, *et al. In vivo* evaluation of a magnesium-based degradable intramedullary nailing system in a sheep model. Acta Biomater, 2015, 25: 369–383
8 Witte F, Hort N, Vogt C, *et al.* Degradable biomaterials based on magnesium corrosion. Curr Opin Solid State Mater Sci, 2008, 12: 63–72
9 Xu W, Birbilis N, Sha G, *et al.* A high-specific-strength and corrosion-resistant magnesium alloy. Nat Mater, 2015, 14: 1229–1235
10 Geddes JR, Burgess S, Hawton K, *et al.* Long-term lithium therapy for bipolar disorder: systematic review and meta-analysis of randomized controlled trials. Am J Psych, 2004, 161: 217–222
11 Baastrup PC, Poulsen JC, Schou M, *et al.* Prophylactic lithium: double blind discontinuation in manic-depressive and recurrent-depressive disorders. Lancet, 1970, 296: 326–330
12 Clément-Lacroix P, Ai M, Morvan F, *et al.* Lrp5-independent activation of Wnt signaling by lithium chloride increases bone formation and bone mass in mice. Proc Natl Acad Sci USA, 2005, 102: 17406–17411
13 Day TF, Guo X, Garrett-Beal L, *et al.* Wnt/β-catenin signaling in mesenchymal progenitors controls osteoblast and chondrocyte differentiation during vertebrate skeletogenesis. Dev Cell, 2005, 8: 739–750
14 Zamani A, Omrani GR, Nasab MM. Lithium's effect on bone mineral density. Bone, 2009, 44: 331–334
15 Hirai K, Somekawa H, Takigawa Y, *et al.* Effects of Ca and Sr addition on mechanical properties of a cast AZ91 magnesium alloy at room and elevated temperature. Mater Sci Eng-A, 2005, 403: 276–280
16 Erdmann N, Angrisani N, Reifenrath J, *et al.* Biomechanical testing and degradation analysis of MgCa0.8 alloy screws: A comparative *in vivo* study in rabbits. Acta Biomater, 2011, 7: 1421–1428
17 Haferkamp H, Niemeyer M, Boehm R, et al. Development, processing and applications range of magnesium lithium alloys. Magnesium alloys, 2000, 350-351: 31–41
18 Haferkamp H, Boehm R, Holzkamp U, *et al.* Alloy development, processing and applications in magnesium lithium alloys. Mater Trans, 2001, 42: 1160–1166
19 Johnston Jr. CC, Miller JZ, Slemenda CW, *et al.* Calcium supplementation and increases in bone mineral density in children. N Engl J Med, 1992, 327: 82–87
20 Tang BM, Eslick GD, Nowson C, *et al.* Use of calcium or calcium in combination with vitamin D supplementation to prevent fractures and bone loss in people aged 50 years and older: a meta-analysis. Lancet, 2007, 370: 657–666
21 Zeng R, Sun X, Song Y, *et al.* Influence of solution temperature on corrosion resistance of Zn-Ca phosphate conversion coating on biomedical Mg-Li-Ca alloys. Trans Nonferrous Met Soc China, 2013, 23: 3293–3299
22 Zeng RC, Sun L, Zheng YF, *et al.* Corrosion and characterisation of dual phase Mg–Li–Ca alloy in Hank's solution: The influence of microstructural features. Corrosion Sci, 2014, 79: 69–82
23 ASTM E8/E8M-16a. Standard Test Methods for Tension Testing of Metallic Materials, Annual Book of ASTM standards. 2004
24 Liu Y, Wu Y, Bian D, *et al.* Study on the Mg-Li-Zn ternary alloy system with improved mechanical properties, good degradation performance and different responses to cells. Acta Biomater, 2017, 62: 418–433
25 Kirkland NT, Birbilis N, Staiger MP. Assessing the corrosion of biodegradable magnesium implants: A critical review of current methodologies and their limitations. Acta Biomater, 2012, 8: 925–936
26 ASTM G31-72. Standard Practice for Laboratory Immersion Corrosion Testing of Metals. 1990
27 Zeng RC, Cui L, Jiang K, *et al. In vitro* corrosion and cytocompatibility of a microarc oxidation coating and poly(l-lactic acid) composite coating on Mg–1Li–1Ca alloy for orthopedic implants. ACS Appl Mater Interfaces, 2016, 8: 10014–10028
28 ISO 10993–5. Biological evaluation of medical devices—Part 5: Tests for *in vitro* cytotoxicity. International Organization for Standardisation, 2009
29 Liu Y, Zhang X, Liu Y, *et al.* Bi-functionalization of a calcium phosphate-coated titanium surface with slow-release simvastatin and metronidazole to provide antibacterial activities and pro-osteodifferentiation capabilities. PLoS ONE, 2014, 9: e97741
30 Ge W, Shi L, Zhou Y, *et al.* Inhibition of osteogenic differentiation of human adipose-derived stromal cells by retinoblastoma binding protein 2 repression of RUNX2-activated transcription. Stem Cells, 2011, 29: 1112–1125
31 Wang Y, Wei M, Gao J, *et al.* Corrosion process of pure magnesium in simulated body fluid. Mater Lett, 2008, 62: 2181–2184
32 Zhang M, Elkin FM. Mg-Li Ultra-light Alloy. Beijing: Science Press, 2010
33 Cipriano AF, Sallee A, Guan RG, *et al.* Investigation of magnesium–zinc–calcium alloys and bone marrow derived mesenchymal stem cell response in direct culture. Acta Biomater, 2015, 12: 298–321
34 Yang C, Yuan G, Zhang J, *et al.* Effects of magnesium alloys extracts on adult human bone marrow-derived stromal cell viability and osteogenic differentiation. Biomed Mater, 2010, 5: 045005
35 Wu Y, Zhu S, Wu C, *et al.* A bi-lineage conducive scaffold for osteochondral defect regeneration. Adv Funct Mater, 2014, 24: 4473–4483
36 Poitevin AA, Viezzer C, Machado DC, *et al.* Effect of standard and neutral-pH peritoneal dialysis solutions upon fibroblasts pro-


  

liferation. J Bras Nefrol, 2014, 36: 150–154
37 Nguyen TY, Liew CG, Liu H. An *in vitro* mechanism study on the proliferation and pluripotency of human embryonic stems cells in response to magnesium degradation. PLoS ONE, 2013, 8: e76547
38 Wang J, Witte F, Xi T, *et al.* Recommendation for modifying current cytotoxicity testing standards for biodegradable magnesium-based materials. Acta Biomater, 2015, 21: 237–249
39 Li Z, Gu X, Lou S, *et al.* The development of binary Mg–Ca alloys for use as biodegradable materials within bone. Biomaterials, 2008, 29: 1329–1344
40 Zhang Y, Xu J, Ruan YC, *et al.* Implant-derived magnesium induces local neuronal production of CGRP to improve bone-fracture healing in rats. Nat Med, 2016, 22: 1160–1169
41 Han P, Wu C, Chang J, *et al.* The cementogenic differentiation of periodontal ligament cells *via* the activation of Wnt/β-catenin signalling pathway by $Li^+$ ions released from bioactive scaffolds. Biomaterials, 2012, 33: 6370–6379
42 Tang L, Chen Y, Pei F, *et al.* Lithium chloride modulates adipogenesis and osteogenesis of human bone marrow-derived mesenchymal stem cells. Cell Physiol Biochem, 2015, 37: 143–152
43 Rude RK, Gruber HE. Magnesium deficiency and osteoporosis: animal and human observations. J Nutritional Biochem, 2004, 15: 710–716
44 Yoshizawa S, Brown A, Barchowsky A, *et al.* Magnesium ion stimulation of bone marrow stromal cells enhances osteogenic activity, simulating the effect of magnesium alloy degradation. Acta Biomater, 2014, 10: 2834–2842
45 Liu Z, Yao X, Yan G, *et al.* Mediator MED23 cooperates with RUNX2 to drive osteoblast differentiation and bone development. Nat Commun, 2016, 7: 11149
46 Komori T. Regulation of osteoblast differentiation by Runx2. Adv Exp Med Biol, 2010, 658: 43–49
47 Neve A, Corrado A, Cantatore FP. Osteocalcin: Skeletal and extra-skeletal effects. J Cell Physiol, 2013, 228: 1149–1153
48 Nakashima K, Zhou X, Kunkel G, *et al.* The novel zinc finger-containing transcription factor osterix is required for osteoblast differentiation and bone formation. Cell, 2002, 108: 17–29
49 Liu F, Kohlmeier S, Wang CY. Wnt signaling and skeletal development. Cellular Signalling, 2008, 20: 999–1009
50 Logan CY, Nusse R. The Wnt signaling pathway in development and disease. Annu Rev Cell Dev Biol, 2004, 20: 781–810
51 Sheng H. Nuclear translocation of beta-catenin in hereditary and carcinogen-induced intestinal adenomas. Carcinogenesis, 1998, 19: 543–549
52 Zhou WR, Zheng YF, Leeflang MA, *et al.* Mechanical property, biocorrosion and *in vitro* biocompatibility evaluations of Mg–Li–(Al)–(RE) alloys for future cardiovascular stent application. Acta Biomater, 2013, 9: 8488–8498
53 Cui L, Sun L, Zeng R, *et al. In vitro* degradation and biocompatibility of Mg-Li-Ca alloys—the influence of Li content. Sci China Mater, 2018, 61: 607–618
54 Díaz-Tocados JM, Herencia C, Martínez-Moreno JM, *et al.* Magnesium chloride promotes osteogenesis through notch signaling activation and expansion of mesenchymal stem cells. Sci Rep, 2017, 7: 7839

**Acknowledgements** This work was supported by the National Key Research and Development Program of China (2016YFC1102900 and 2016YFC1102402), the National Natural Science Foundation of China (81771039, 81470769 and 51431002), the Project for Culturing Leading Talents in Scientific and Technological Innovation of Beijing, China (Z171100001117169), the NSFC-RFBR Cooperation Project (51611130054), and the NSFC/RGC Joint Research Scheme (51361165101 and 5161101031).

**Author contributions** Xia D and Liu Y designed and performed the experiments with assistance from Zheng Y and Liu Y; Zheng Y and Liu Y supervised the project; Xia D prepared the manuscript; Wang S performed the data analysis; Zeng R and Zhou Y contributed in language improvements and proof reading. All authors have given approval to the final version of the manuscript.

**Conflict of interest** The authors declare that they have no conflict of interest.

**Supplementary information** Supporting data are available in the online version of the paper.

  

**Dandan Xia** is currently a PhD student at the School and Hospital of Stomatology, Peking University. She received her Bachelor's degree from Peking University in 2015. Her research focuses on the magnesium alloys and mesenchymal stem cells.

**Yunsong Liu** received his PhD in the School and Hospital of Stomatology from Peking University, China, in 2008. Since 2008, he has been a full professor at Peking University in Beijing, China. His research focuses on the magnesium alloys and mesenchymal stem cells.

**Yufeng Zheng** received his PhD in materials science from Harbin Institute of Technology, China, in 1998. Since 2004, he has been a full professor at Peking University in Beijing, China. His research focuses on the development of various new biomedical metallic materials (biodegradable Mg, Fe and Zn based alloys, β-Ti alloys with low elastic modulus, bulk metallic glass, ultra-fine grained metallic materials, etc.).

## 镁锂钙合金作为骨植入材料的体内外研究

夏丹丹[1], 刘洋[2], 王思仪[1], 曾荣昌[3], 刘云松[1,4*], 郑玉峰[2*], 周永胜[1,4]

**摘要** 本文制备了三元Mg-(3.5, 6.5 wt.%)Li-(0.2, 0.5, 1.0 wt.%)Ca合金, 并研究了其力学性能、腐蚀性能与生物相容性. 此合金的力学性能较纯镁显著提高, 并具有良好的耐腐蚀性. 然后, 将体外性能最佳的Mg-3.5Li-0.5Ca合金植入小鼠股骨骨髓腔, 体内实验结果显示, Mg-3.5Li-0.5Ca合金周围的骨厚度增加, 未见不良反应. Western blot和免疫荧光染色结果显示, Mg-3.5Li-0.5Ca合金通过经典的Wnt/β-catenin信号通路促进了人骨髓间充质干细胞的成骨向分化. 研究结果表明, Mg-3.5Li-0.5Ca合金具有作为骨植入材料的巨大潜力.

  